Predictability of the 2020 Antarctic strong vortex event and the role of ozone forcing

Eun-Pa Lim[1], Linjing Zhou[1], Griffith Young[1], S. Abhik[2], Irina Rudeva[1], Pandora Hope[1], Matthew C. Wheeler[1], Julie M. Arblaster[3], Harry H. Hendon[3], Gloria L. Manney[4,5], Seok-Woo Son[6], Jiyoung Oh[7]

[1] Bureau of Meteorology, Melbourne, Victoria, Australia

[2] School of Earth, Atmosphere and Environment, Monash University, Clayton, Victoria, Australia

[3] Securing Antarctica′s Environmental Future, School of Earth, Atmosphere and Environment, Monash University, Clayton, Victoria, Australia

[4] NorthWest Research Associates, Socorro, New Mexico, USA

[5] Department of Physics, New Mexico Institute of Mining and Technology, Socorro, New Mexico, USA

[6] School of Earth and Environmental Sciences, Seoul National University, Seoul, Republic of Korea

[7] Korea Meteorological Administration, Seoul, Republic of Korea

Corresponding author: Eun-Pa Lim, eun-pa.lim@bom.gov.au

Key points

- The Antarctic vortex of 2020 was the strongest event in the satellite era for the October-December mean in the mid- to lower stratosphere
- Its unusual dynamical evolution limited its predictability to less than a month
- Realistic ozone forcing could significantly improve forecasts for the 2020 polar vortex strength and its downward impact

Abstract

In the austral spring seasons of 2020-2022, the Antarctic stratosphere experienced three consecutive strong vortex events. In particular, the Antarctic vortex of October-December 2020 was the strongest on record in the satellite era for that season at 60°S in the mid- to lower stratosphere. However, it was poorly predicted by the Australian Bureau of Meteorology's operational seasonal climate forecast system of that time, ACCESS-S1, even at a short lead time of a month. Using the current operational forecast system, ACCESS-S2, we have, therefore, tried to find a primary cause of the limited predictability of this event and conducted forecast sensitivity experiments to climatological versus observation-based ozone to understand the potential role of the ozone forcing in the strong vortex event and associated anomalies of the Southern Annular Mode (SAM) and south-eastern Australian rainfall. Here, we show that the 2020 strong vortex event did not follow the canonical dynamical evolution seen in previous strong vortex events in spring, whereas the ACCESS-S2 control forecasts with the climatological ozone did, which likely accounts for the inaccurate forecasts of ACCESS-S1/S2 at 1-month lead time. Forcing ACCESS-S2 with observed ozone significantly improved the skill in predicting the strong vortex in October-December 2020 and the subsequent positive SAM and related rainfall increase over south-eastern Australia in the summer of December 2020 to February 2021. These results highlight an important role of ozone variations in seasonal climate forecasting as a source of long-lead predictability, and therefore, a need for improved ozone forcing in future ACCESS-S development.

Plain Language Summary

In the spring seasons of 2020-2022, the Antarctic stratosphere experienced three strong vortex events. In particular, the Antarctic vortex of October-December 2020 was the strongest on record in the satellite observation era for that season when monitored at 60°S in the mid- to lower stratosphere (altitudes of 15-30 km). However, this super vortex event was poorly predicted by the Australian Bureau of Meteorology's operational seasonal climate forecast system even at 1-month lead time. Our analysis reveals that the dynamical evolution of the 2020 polar vortex was highly unusual compared to those of the previous strong vortex events, which likely explains its lack of long-lead predictability. The forecast model experiments prescribed with observed versus unrealistic ozone forcing show that using the observed ozone, characterized by a significant loss over Antarctica in spring 2020, resulted in the forecast improvements for the 2020 super vortex strength and the associated poleward shift of the Southern Hemisphere (SH) midlatitude jet in the lower atmosphere and anomalously wet conditions over south-eastern Australia in summer. These results highlight a need to improve representations of ozone forcing in dynamical sub-seasonal to seasonal climate forecast systems to better predict the year-to-year variability of the SH surface climate conditions.

1. Introduction

The Antarctic stratospheric polar vortex (also referred to as the polar vortex in this study) is a planetary-scale cyclonic circulation encircling the South Pole from austral autumn to spring. Its maximum westerly wind speed is found in the latitude band of 40-50°S near the stratopause (~1 hPa level) in winter (Andrews et al., 1987), and as the season progresses through spring, it gradually weakens with poleward and downward movements as a result of vigorous wave-mean flow interactions (e.g., Matsuno 1970; Hartmann et al. 1984; Randel and Newman 1998). Eventually, the westerly vortex breaks down sometime in November to December in the upper to mid-stratosphere (Black & McDaniel, 2007; Hio & Yoden, 2005; Kuroda & Kodera, 1998).

The interannual variability of the Antarctic stratospheric vortex peaks in the upper to mid-stratosphere in October and is often the expression of different paces of the seasonal march of the vortex (e.g., Shiotani et al. 1993; Byrne and Shepherd 2018). Active feedback between planetary-scale waves and vortex winds on latitudinal and vertical critical lines (where the phase speeds of waves equal the background zonal wind speeds) leads to poleward and downward movements of the anomalous wind, temperature, and pressure around and over the Antarctic region (e.g., Kuroda and Kodera 1998; Hio and Yoden 2005; Shaw et al. 2010; Byrne and Shepherd 2018; Lim et al. 2018). The downward coupling of the stratospheric anomalies with some time lag makes the Antarctic stratospheric vortex variability during spring and early summer an important source of predictability of the state of the tropospheric Southern Annular Mode (SAM) (e.g., Kidson 1988; Gong and Wang 1999; Thompson and Wallace 2000; Marshall 2003); which, in turn, significantly impacts Southern Hemisphere (SH) surface weather and climate as well as associated oceanic circulations and sea-ice extent (e.g., Silvestri and Vera 2003; Reason and Rouault 2005; Sen Gupta and England 2006; Gillett et al. 2006; Hendon et al. 2007, 2014; Stammerjohn et al. 2008; Harris and Lucas 2019; Lim et al. 2019; Wang et al. 2019; Hartmann 2022). For instance, when the seasonal march of the vortex evolution is accelerated, the spring polar vortex weakens and warms earlier than usual. Weaker and warmer polar vortices can lead to unusually high Antarctic ozone concentrations, which further warm the Antarctic region, and consequently result in the SAM to be in its negative phase in spring through early summer (e.g., years 2002, 2019) (Stolarski et al. 2005; Byrne and Shepherd 2018; Lim et al. 2018; Noguchi et al. 2020). The opposite chain of processes occurs when the seasonal march of the vortex evolution is decelerated, and the spring vortex is unusually strong and cold and breaks down later than usual (Limpasuvan et al., 2005).

Previous studies noted that the interannual variability of the Antarctic stratospheric vortex has significantly increased since 2000 (E.-P. Lim et al., 2018; Shen et al., 2022), a period when the Inter-decadal Pacific Oscillation has been in its cold phase (e.g., Yuan Zhang et al. 1997; Kosaka and Xie 2013; Henley et al. 2015) and a plateauing or weak recovery of the Antarctic ozone depleting trend has been detected (e.g., Salby et al. 2011; Solomon et al. 2016; Stone et al. 2021). In particular, the springtime Antarctic polar vortex experienced its full swing from a near-record/record-breaking vortex weakening and warming event in 2019 to three consecutive strong and cold vortex events in 2020-2022 (e.g., Rao et al. 2020; Shen et al. 2020; Wargan et al. 2020; Lim et al. 2021; Yook et al. 2022). The strong and persistent 2020 vortex in late spring was especially noteworthy as it was the strongest and coldest event since at least 1979 in the mid- to lower stratosphere for the October to December mean (Figs. 1a,b). The Antarctic ozone concentration was also significantly lower than normal during that season (Fig. 1c), as expected from the exceptionally strong and more persistent polar vortex (e.g.,

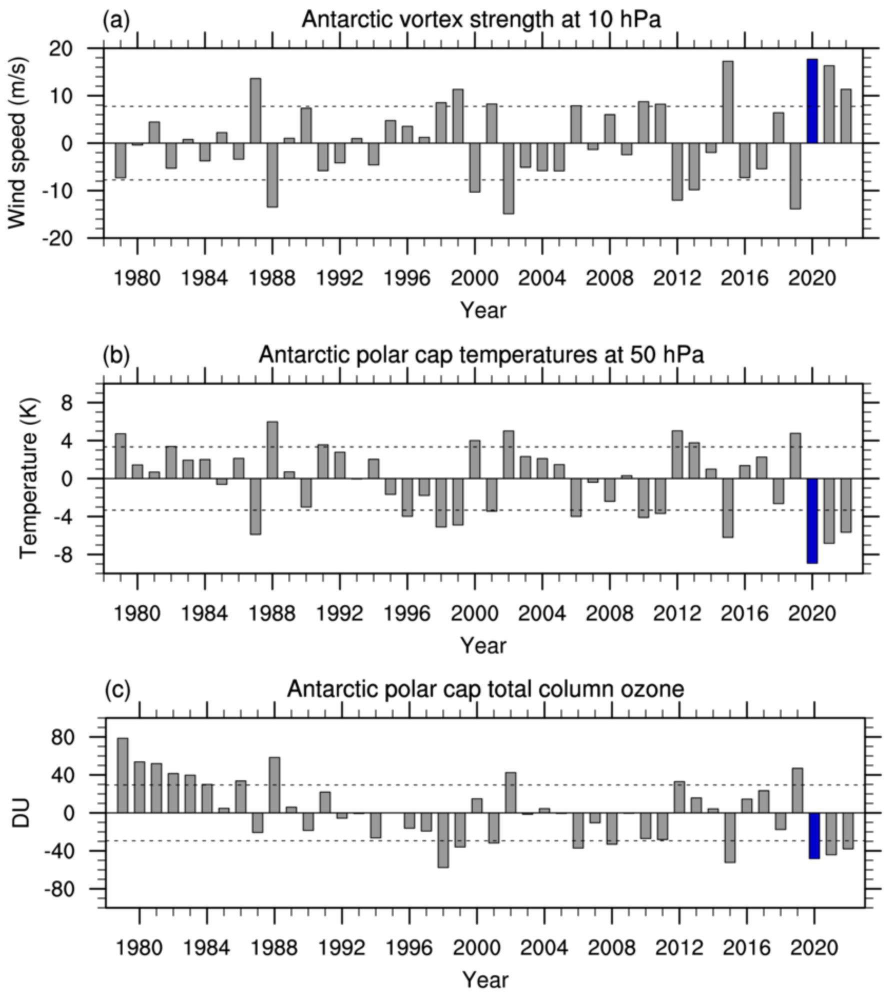

Figure 1. (a) Time series of the October-December mean stratospheric polar vortex wind anomalies as monitored by zonal-mean zonal wind anomalies ([U]') relative to the climatology of 1981-2018 at 60°S and 10 hPa. (b) The same as (a) but temperature anomalies averaged over the Antarctic polar cap region poleward of 60°S at 50 hPa. (c) The same as (a) but total column ozone anomalies averaged over the Antarctic polar cap region poleward of 63°S. The 2020 anomalies are marked by the blue-colored bars. The horizontal lines denote ±1 standard deviation (σ). The wind and temperature data are from the JRA-55 reanalysis (Kobayashi et al., 2015) and the ozone data are from the NASA Ozone Watch (https://ozonewatch.gsfc.nasa.gov/SH.html).

Randel and Newman 1998; Seviour et al. 2014; Lim et al. 2018). Although this low polar cap ozone anomaly came after an unusual wintertime ozone depletion in the lower latitudes of the SH caused by the Australian Black Summer (or Australian New Year's) bushfire smoke of late 2019 to early 2020 (Rieger et al. 2021; Yu et al. 2021; Santee et al. 2022; Solomon et al. 2023), the studies of Santee et al. (2022) and Solomon et al. (2023) indicate that the austral springtime ozone loss of 2020 over Antarctica did not result from the smoke.

Despite its record strength, the 2020 super vortex event was not well predicted by the Bureau of Meteorology (BoM)'s operational dynamical sub-seasonal to seasonal (S2S) climate forecast system, ACCESS-S1 (the Australian Community Climate and Earth System Simulator – Seasonal version 1; Hudson et al. 2017), until the beginning of October 2020, by which time the anomalously strong vortex condition had already persisted for a month (Fig. 2). The lack of long-lead predictability of this super vortex event was puzzling because dynamical S2S forecast systems demonstrate useful skill in predicting the SH spring stratospheric polar vortex from July when assessed over their hindcast periods of 20-40 years (E. P. Lim et al., 2021; Wedd et al., 2022). Consistent with the hindcast skill, ACCESS-S1 and S2 skilfully predicted the 2021 and 2022 Antarctic strong vortex events of October-December, respectively, at 2-month lead time from early August (Supplementary Fig. S1). One contributor to the poor forecast performance for the 2020 vortex event could be that the forecasts were forced by prescribed unrealistic ozone concentrations (i.e., the monthly climatological ozone as a common forecast practice) (e.g., Seviour et al. 2014; Hendon et al. 2020; Oh et al. 2022) rather than being forced by dynamically balanced more realistic ozone concentrations (e.g., as simulated by an interactive chemistry-climate model; Fogt et al. 2009, Friedel et al. 2022). In this study, we aim to understand i) some key characteristics of the 2020 super vortex event that could be related to its lack of predictability at a lead time as short as 1 month; and ii) the role of the ozone forcing in the strength of the polar vortex and its downward impact on the surface SAM and associated Australian rainfall, which should highlight the interannual variability of ozone as a potential source of predictability of this strong vortex event and associated SH surface climate anomalies.

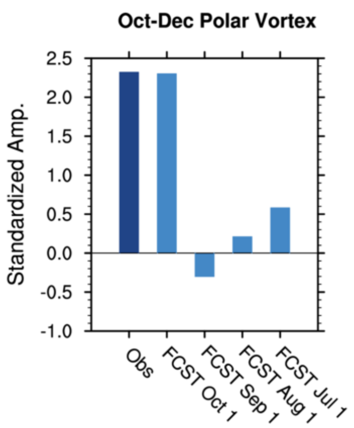

Figure 2. ACCESS-S1 11- member ensemble mean forecasts for the October-December mean stratospheric polar vortex ([U]' at 60°S, 10 hPa) when forecasts were initialised on 1 October (lead time 0), 1 September (lead time 1 month), 1 August (lead time 2 months), and 1 July (lead time 3 months) of 2020 (light blue bars). The dark blue bar indicates the observed strength of the 2020 vortex. The observed and forecast standardized anomalies were obtained relative to their respective climatological means and standard deviations of 1990-2012 (when ACCESS-S1 hindcasts are available).

2. Data, forecast system, and experimental design

To address the above research questions, we have conducted forecast sensitivity experiments to climatological *vs.* realistic 2020 ozone forcing, using the BoM's S2S forecast system, ACCESS-S2, which replaced ACCESS-S1 as the operational system in October 2021 (Wedd et al. 2022). ACCESS-S2 is an atmosphere-land-ocean-sea-ice fully coupled dynamical forecast system. Its model is based on the UK Met Office GloSea5-GC2 seasonal prediction system (MacLachlan et al., 2015) and is identical to ACCESS-S1 except for minor corrections and enhancements, including a correction in the atmospheric model code that reads ozone data to follow a 365-day calendar instead of a 360-day calendar (Hendon et al., 2020; Wedd et al., 2022). The model's horizontal resolution is 25 km in the ocean and ~60 km in the atmosphere in the midlatitudes (N216). The vertical resolution of the atmospheric model (the Unified Model version 8.6; Walters et al. 2017) is 85 levels with a well-resolved stratosphere (35 levels above 18 km). The main difference between ACCESS-S1 and ACCESS-S2 is that ACCESS-S2 is initialized using the BoM's weakly-coupled ensemble optimum interpolation data assimilation scheme for the ocean, sea-ice, and land surface (Wedd et al., 2022). In contrast, ACCESS-S1 was initialized with the UK Met Office Forecast Ocean Assimilation Model (FOAM) analysis data (J. Waters et al., 2015). The ocean initial conditions for ACCESS-S2 are available for 1981-2018 and October 2021 onwards. Due to the unavailability of these new conditions for 2020, we used the UK Met Office FOAM analysis data (J. Waters et al., 2015) to initialise our experiments. The atmospheric initial conditions come from the BoM's 4-D Var data assimilation analyses for 2020 (Bureau of Meteorology, 2019) and the European Centre for Medium-Range Weather Forecasts (ECMWF)-Interim reanalysis (ERA-Interim; Dee et al. 2011) for the hindcasts (retrospective forecasts) for 1981-2018.

For this study, we generated 3-member hindcasts for 1981-2018 to compute the forecast climatology and 33-member ensemble forecasts for 2020 by perturbing the atmospheric initial conditions (Hudson et al. 2017; Wedd et al. 2022). These forecasts were forced with prescribed monthly *climatological* zonal-mean ozone averaged over 1994-2005 (Cionni et al., 2011), the same as the operational configuration of ACCESS-S2 (and ACCESS-S1) for ozone forcing. We refer to these standard forecasts as the “control” forecasts. To understand the role of the 2020 ozone forcing in the strength of the polar vortex and its downward impacts, we generated a second set of 33-member ensemble forecasts forced with the prescribed *2020 observed* monthly zonal-mean ozone from the ECMWF Reanalysis version 5 (ERA5; Hersbach et al. 2020). ERA5 assimilates more and higher quality observational data compared to its predecessor (Dee et al., 2011), including assimilation of Aura Microwave Limb Sounder (J. W. Waters et al., 2006) Ozone Profiles and Ozone Monitoring Instrument column ozone (Levelt et al., 2006), which provide near-global daily coverage. ERA5 stratospheric ozone has been demonstrated to be accurate by comparisons with observational data and other reanalyses (e.g., SPARC 2022, Chapter 4). The ERA5 ozone anomalies for 2020 were computed relative to the ERA5 climatology of 1994-2005 and then added to the ozone climatology used for the control forecasts throughout all vertical levels. These forecasts are referred to as the "experimental" forecasts.

All forecasts were initialized on 1 September 2020 and verified from September 2020 to February 2021. The forecasts are verified against the JRA-55 data (the Japanese 55-year ReAnalysis; Kobayashi et al. 2015). The JRA-55 reanalysis dataset has been shown to be of high quality for dynamics studies such as those herein (e.g., SPARC, 2022, Chapter 6). However, it does not do inline ozone assimilation (Hersbach et al., 2020). The rainfall forecasts over Australia are verified against the BoM's Australian Gridded Climate Data (AGCD; Jones et al. 2009; Evans et al. 2020).

3. Characteristics of the observed 2020 super vortex event and ozone anomalies

Year-to-year variability of the polar vortex in the reanalysis data is identified by an empirical orthogonal function (EOF) analysis (North et al., 1982) applied to the zonal-mean zonal wind anomalies ([U]') at 60°S over the domain of vertical (pressure) levels and calendar months (Figs. 3a,b) (e.g., Hio and Yoden 2005; Lim et al. 2018). The interannual variability is characterized by persistent anomalies during spring and early summer throughout the stratosphere and the troposphere, with a maximum anomaly in the mid- to upper stratosphere in October. These anomalies, when positive, are related to a delay of the vortex breakdown in the upper to mid-stratosphere (and an earlier breakdown when negative). The other notable feature in Figure 3b is the oppositely signed wind anomalies in the upper stratosphere during the austral winter months that precede wind anomalies of spring and early summer.

Dynamical processes associated with this abrupt change of upper stratospheric zonal wind anomalies at around 60°S from winter to spring can be understood by examining the zonal wind anomalies at 1 hPa regressed to the temporal coefficients of the EOF pattern (Fig. 3a) displayed as a function of the latitude and calendar months (Fig. 3c). The regression plot shows that the negative zonal wind anomalies at 60°S in June and July displayed in Figure 3b are associated with an equatorward shift of the winter jet in the upper stratosphere as marked by the meridional dipole anomalies centered on the jet. The dipole anomalies of the winter jet gradually move poleward with time as a result of active interactions with the upward and equatorward propagation of planetary-scale waves and associated wave breaking at the critical latitudes (e.g., Hartmann et al. 1984; Kuroda and Kodera 1998; Polvani and Waugh 2004; Lim et al. 2018, 2021; Baldwin et al. 2021). This wave-mean flow feedback that

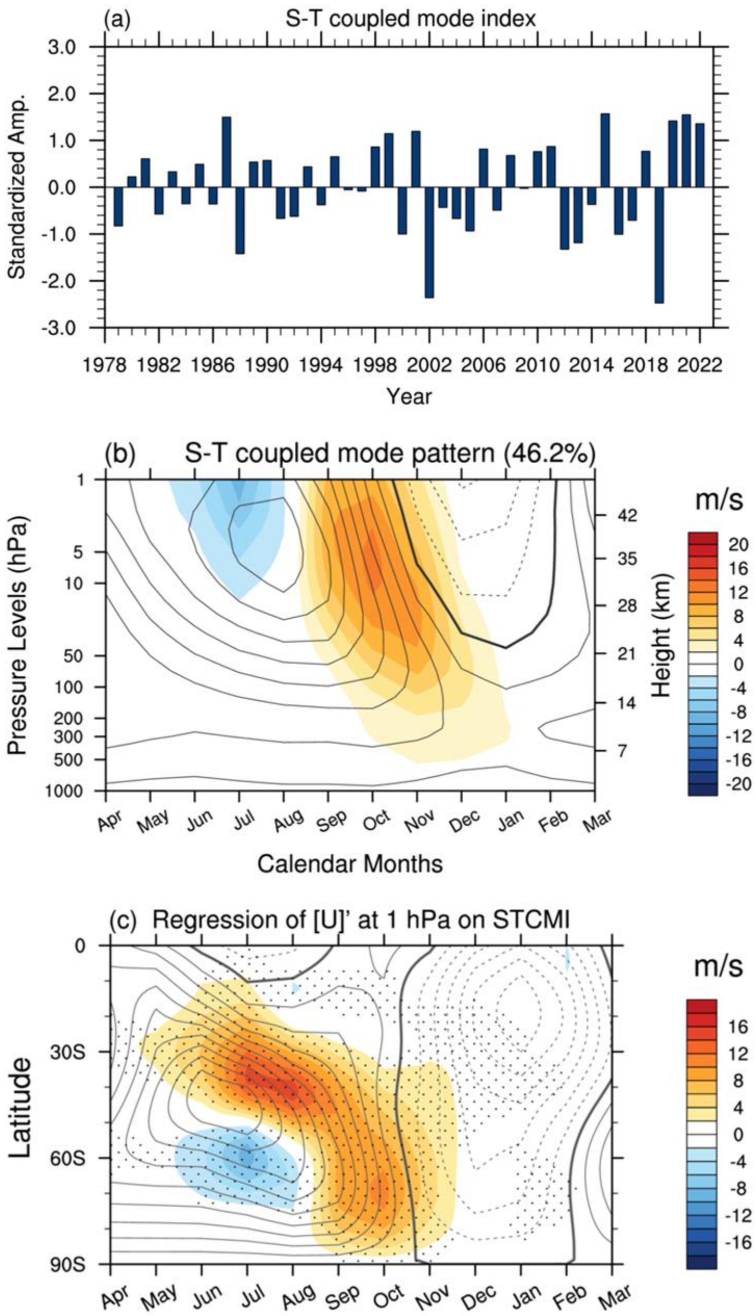

Figure 3. The stratosphere-troposphere (S-T) coupled mode captured by the first mode of a height-time domain EOF analysis applied to the monthly mean zonal mean-zonal wind anomalies ([U]') at 60°S over 1979-2022. (a) The S-T coupled mode temporal coefficient time series (S-T coupled mode index; STCMI), (b) the S-T coupled mode eigenvector (EOF1), and (c) regression of [U]' at 1 hPa onto the STCMI displayed in (a) (regression coefficients were scaled by 1σ of the STCMI to preserve the wind unit). The contours in (b) and (c) indicate the 1981-2018 climatology of [U] at 60°S and [U] at 1 hPa, respectively. The thin-solid, thick-solid and thin-dashed lines indicate positive, zero and negative zonal mean winds, respectively. The contour interval is 10 ms^{-1}. Stippling in (c) denotes statistically significant regression coefficients at the 90% confidence level, as assessed by a two-tailed student t-test with 44 samples.

leads to a spring polar vortex anomaly can be summarized by simple statistical relationships as shown in Lim et al. (2021): the June-July mean westerly wind anomalies at 60°S and 1 hPa are positively correlated with the July-August mean upward propagating wave activities represented by the poleward eddy heat flux (-v'T' in the SH) anomalies averaged over 45-75°S at 100 hPa (correlation coefficient, *r* ~ 0.5). These late winter wave activities are, in turn, anti-correlated with the September-November mean [U]' at 60°S and 10 hPa (*r* ~ -0.6). Consequently, the spring zonal wind anomalies are anti-correlated with the early winter westerly anomalies at 60°S and 1 hPa (*r* ~ -0.6), as depicted in Figure 3b. Because of these time-lagged relationships, the winter jet dipole anomalies in the upper stratosphere and the upward propagating wave activity anomalies in the lower stratosphere are important precursors that serve as sources of predictability of the springtime polar vortex condition (e.g., Shiotani et al. 1993; Polvani and Waugh 2004). Thus, an unusually strong springtime polar vortex often follows from stronger wintertime westerlies in midlatitudes and weaker westerlies in high latitudes at the top of the stratosphere (i.e., an equatorward shift of the winter upper-stratospheric jet; Shiotani et al. 1993). Such changes in the zonal winds tend to discourage planetary-scale waves propagating into the stratosphere during winter months (as measured by reduced poleward heat flux at 100 hPa in the SH) (Fig. 4a).

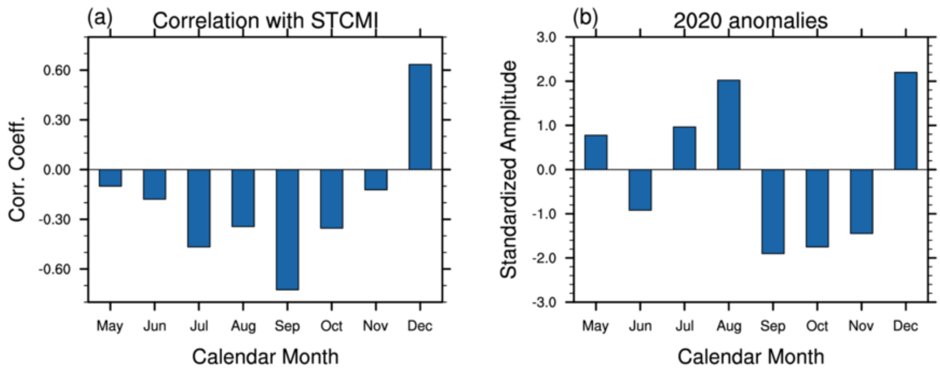

Figure 4. (a) Correlation of poleward eddy heat flux detected at 100 hPa with the STCMI displayed in Figure 3a. Negative correlation means less heat is transported poleward and upward (i.e., reduced upward propagating wave activity) in relation to the stronger-than-normal zonal winds in spring to early summer. (Note that in the SH, the *poleward* heat flux is computed as *-v'T'* where *v'* and *T'* are the eddy components of meridional wind and temperature, respectively - i.e., *negatively signed northward* heat flux). 0.3 correlation is statistically significant at the 95% confidence level as assessed by a two-tailed student t-test with 44 samples from 1979-2022. (b) Monthly mean anomalies of 2020 poleward eddy heat flux.

In comparison to this canonical process, in 2020 the stronger-than-normal zonal-mean zonal winds around 60°S in the upper stratosphere were extraordinarily persistent from May until December (Fig. 5a). The westerly anomalies of the vortex in the upper stratosphere in July showed signs of a decrease in August and September. However, they increased again from October, in contrast to the typical evolution of the polar vortex, which would be a continuing decrease of the westerlies in spring (as implied in Figure 3b). Further, the vortex wind anomaly of 2020 peaked in November in the mid-stratosphere, later in time and lower in altitude than the variability maximum. The unusually strong vortex wind anomalies were accompanied by significant cold anomalies in the Antarctic vortex (Fig. 5b). The unconventional dynamical evolution of this super vortex event is also apparent in the latitude-time plot of the 2020 [U]' at 1 hPa in Figure 5c. The winter stratospheric jet had easterly anomalies on its equatorward side and westerly anomalies on its poleward side, suggesting a poleward shift of the jet (i.e., poleward shrinking of the vortex), which would generally lead to spring polar vortex weakening as implied in Figure 3c (with the opposite signs). Consistent with this poleward winter jet shift, there was an increase in the poleward eddy heat flux in the lower stratosphere in July and August (Fig. 4b), which implies increased heat transport toward the polar region and upward propagating wave activities that would act to weaken the polar vortex in spring. Therefore, the wintertime winds and wave forcing in 2020 appeared favorable for an anomalous weakening of the springtime polar vortex, which suggests that the unusual vortex strength in October-December was unlikely to be the result of canonical dynamical forcing that typically comes from the upper stratosphere in winter (E.-P. Lim et al., 2018; E. P. Lim et al., 2021). In contrast, the upper stratospheric dynamical evolution of the unusually strong vortices of October-December 2021 and 2022 was consistent with that historically associated with stronger-than-normal spring polar vortices, as shown in Figure 3c (Fig. S2).

Although the unusually strong polar vortex of 2020 occurred without an obvious dynamical precursor, its wind and temperature anomalies moved downward to the surface in a typical manner, thereby likely contributing to the positive SAM that developed in the late spring and summer months of November-February, when the 2020-21 La Niña would have also played a role in promoting a positive SAM (e.g., L'Heureux and Thompson 2006; Lim and Hendon 2015; Fogt and Marshall 2020) (Fig. 6). The positive SAM was likely a key driver of the unusually wet conditions over south-eastern Australia during austral summer 2020-21, given its resemblance to the historical response of the summer rainfall to the positive SAM (e.g., Hendon et al. 2007; Fig. 7). On the other hand, the excessive rainfall over northern and western Australia was likely driven by La Niña combined with a long-term tropical SST trend (e.g., McBride and Nicholls 1983; Risbey et al. 2009; Lim et al. 2016; Sharmila and Hendon 2020; Heidemann et al. 2023).

As briefly discussed in the introduction, the Antarctic ozone in the lower stratosphere was significantly less than normal from September 2020 to the following year's January, reflecting the ozone being extensively depleted in early spring by the unusually strong and cold polar vortex and then staying confined within the vortex until the vortex broke down in early summer (Fig. 8a). Near the tropopause, the lower-than-usual Antarctic ozone concentration appears to have lingered at least until March 2021. Also, the anomalous ozone depletion in winter 2020 in the midlatitudes near 30-50°S is apparent at 50 hPa (Fig. 8b), which has been under debate for its partial attribution to the aerosol loading by the Australian Black Summer bushfire smoke injection into the stratosphere (e.g., Santee et al. 2022; Solomon et al. 2023). While the magnitudes of the midlatitude ozone anomalies were moderate, they were greater than 1 standard deviation estimated over the climatological period of 1981-2018. The impact of the polar and mid-latitude zonal-mean ozone anomalies in 2020 on the Antarctic circulation and temperature anomalies in the spring and summer of 2020-2021 will be examined in the next section using forecast experiments testing the sensitivity to climatological *vs.* realistic ozone forcing.

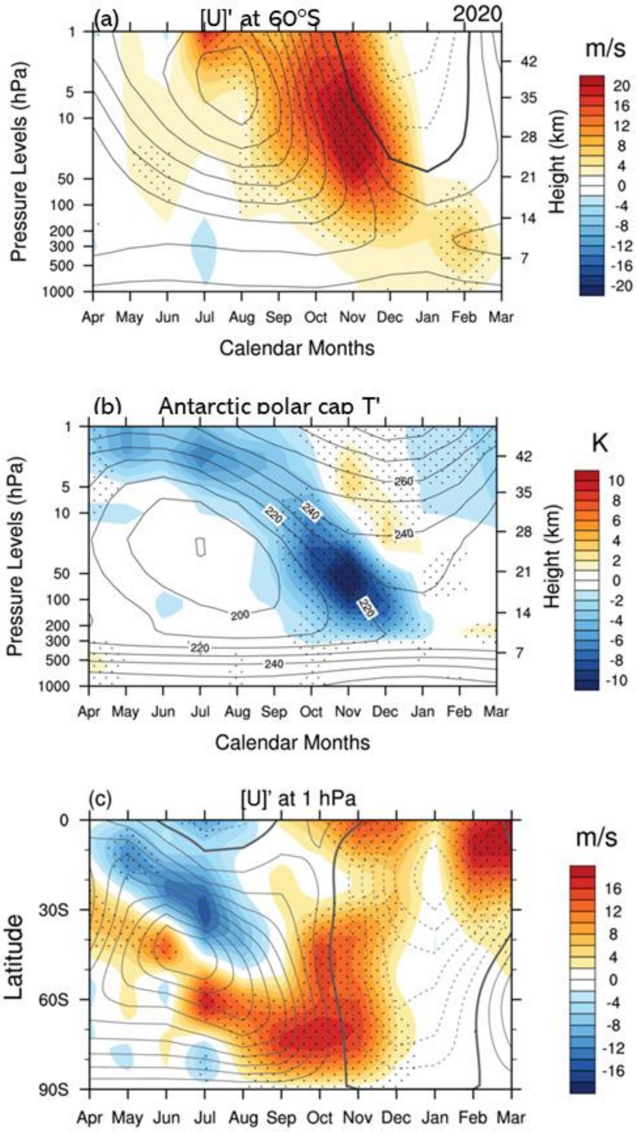

Figure 5. 2020 monthly mean anomalies of (a) zonal-mean zonal winds at 60°S, (b) the Antarctic polar cap temperatures averaged over 60-90°S with cosine latitude weighting, and (c) zonal-mean zonal winds at 1 hPa. Contours indicate the 1981-2018 climatologies with 10 ms^{-1} and 10 K intervals for (a), (c) and (b), respectively. Stippling indicates the magnitude of 2020 anomalies greater than 1σ estimated over the climatological period. Wind and temperature data were de-trended before plotting, but de-trending did not make any significant difference.

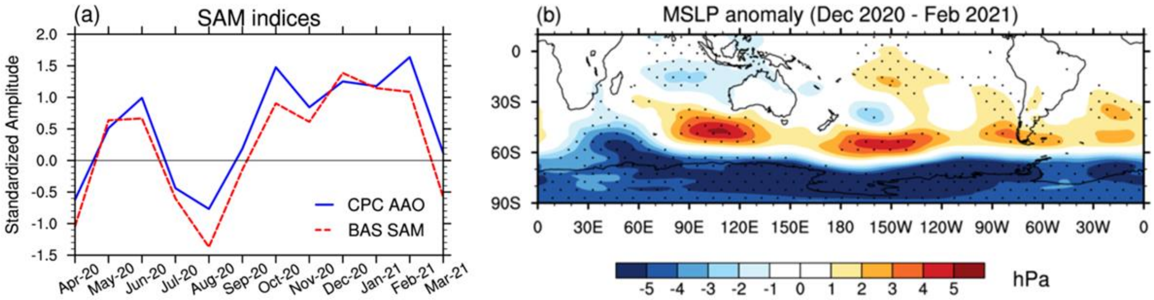

Figure 6. (a) Standardized amplitude of the SAM from April 2020 to March 2021 monitored by the NOAA Climate Prediction Center Antarctic Oscillation index (CPC AAO; Thompson and Wallace 2000) and the British Antarctic Survey's SAM index (BAS SAM; Marshall 2003). (b) Mean sea level pressure (MSLP) anomalies averaged over the period from December 2020 to February 2021 (DJF 2020-21). Stippling indicates the magnitude of the 2020 anomalies greater than 1σ estimated over the climatological period.

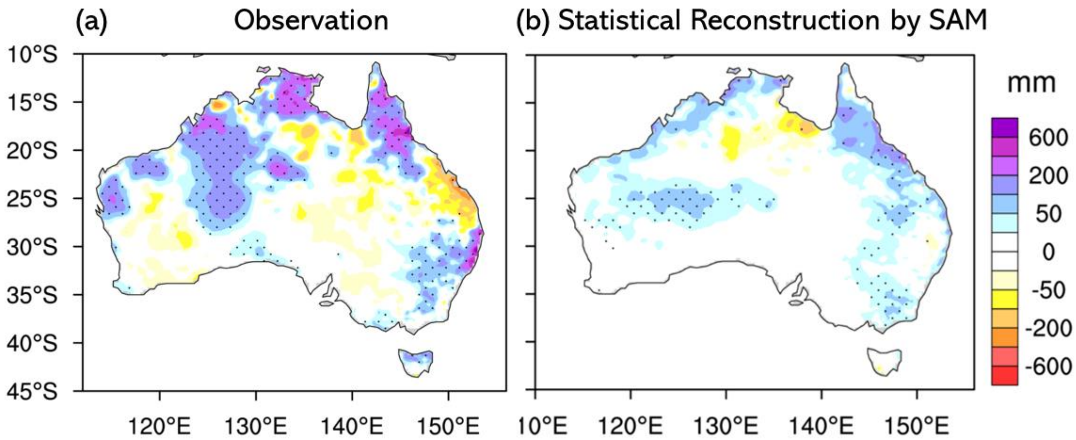

Figure 7. (a) DJF 2020-21 rainfall anomalies over Australia relative to the climatological mean of 1981-2018. Stippling indicates the magnitude of the rainfall anomalies greater than 1σ estimated over the climatological period. (b) Reconstructed rainfall anomalies of DJF 2020-21 by regressing the DJF rainfall onto the CPC AAO index for the period of 1981-2018 and scaling the resultant regression coefficient by the amplitude of the AAO index in DJF 2020-21 (1.79σ). Stippling indicates the statistical significance on the regression coefficients at the 90% confidence level, estimated by a two-sided student t-test, given 38 samples.

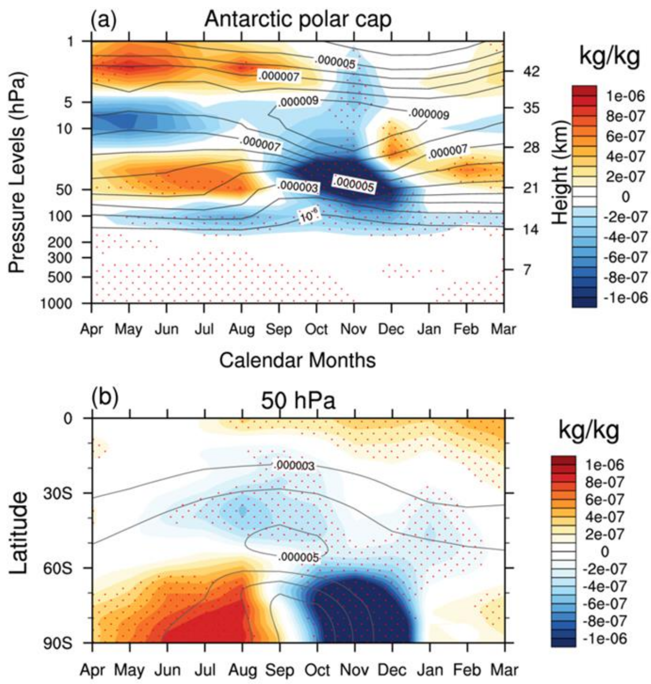

Figure 8. ERA5 ozone anomalies (a) over the Antarctic polar cap region of 60-90°S displayed as a function of pressure level and calendar month and (b) in the lower stratosphere at 50 hPa displayed as a function of latitude and calendar month. Contours indicate the 1981-2018 climatologies of the respective fields. In the calculation of the climatologies, the ERA5 data for 2000-2006 were replaced by those of the ERA5.1 where lower stratosphere cold biases and unrealistic spikes of ozone close to the South Pole in the winter months of 2003-2004 were fixed (Simmons et al., 2020). Red-coloured stippling indicates the magnitude of the 2020 anomalies greater than 1σ estimated over the climatological period.

4. ACCESS-S2 forecast experiments with two different ozone forcings

4.1 Control forecasts with the climatological ozone forcing

ACCESS-S2 has statistically significant skill in predicting [U]' at 60°S and 10 hPa for the spring and summer seasons in the hindcast period of 1990-2012 at up to 4-month lead time (Wedd et al. 2022). For the October-December mean [U]' at 60°S and 10 hPa for the 1981-2018 climatological period used in this study, the predictive skill of ACCESS-S2 is high with ~0.7 correlation at 1-month lead time (i.e., forecasts initialized on 1 September and verified for the October-December mean) and remains above the statistically significant level of 95% (> 0.33 correlation with 38 samples) at up to 3-month lead time (i.e., forecasts initialized on 1 July) (Fig. S3).

Despite the demonstrated hindcast skill, the 2020 strong vortex event of October-December was not skilfully captured by the ensemble mean of ACCESS-S2 with the climatological ozone forcing (control forecasts) at a relatively short lead time of 1 month (Fig. 9a). At this lead time, the model did simulate an unusually cold polar stratosphere and unusually strong westerlies for late spring to summer, but the predicted cooling was too mild and the stratospheric wind anomalies were delayed by 2 months compared to those in the reanalysis (Figs. 9a,b; *cf.*, Figs 5a,b). The latitude-time evolution of the upper stratospheric [U]' suggests that the forecast stratospheric winds followed the canonical poleward evolution of the meridional dipole anomalies of the winter stratospheric jet (Fig. 9c), as depicted by the regression pattern to the stratosphere-troposphere coupled mode index but with the opposite sign (Fig. 3c). That is, the midlatitude easterly anomalies (flanked by high latitude westerly anomalies) in the initial conditions of early September were forecast to migrate to the pole by October, which did not happen in reality in 2020 (Fig. 5c).

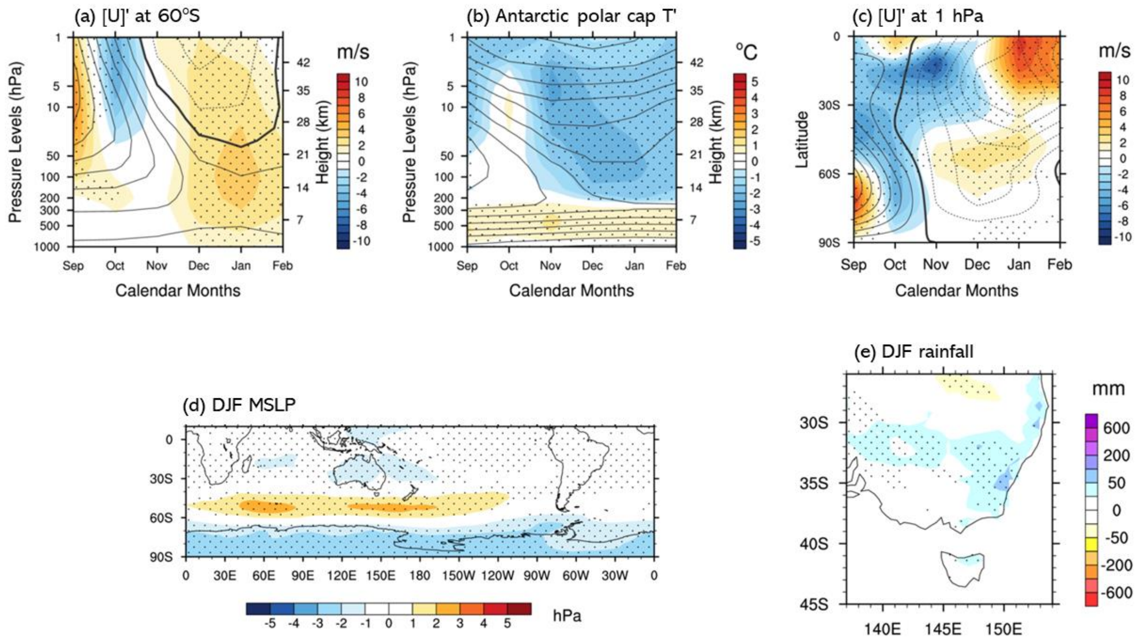

Figure 9. Control forecasts with the climatological ozone forcing for (a) [U]' at 60°S, (b) the Antarctic polar cap averaged T', (c) [U]' at 1 hPa, (d) DJF mean MSLP anomalies, and (e) DJF mean rainfall anomalies of 2020-2021. The contours in (a)-(c) indicate the ACCESS-S2 climatologies of the relevant fields computed over 1981-2018. The contour interval is 10 ms^{-1} in (a) and (c) and 10 K in (b). Stippling indicates the statistically significant anomalies at the 90% confidence level as assessed by a two-tailed student t-test with 33 samples of the control forecast set and 3 (ensemble members) x 38 (hindcast years) samples of the hindcast set.

In addition, the control forecasts predicted the maximum westerly anomalies in the troposphere rather than in the stratosphere during summer (Fig. 9a; *cf.* Fig. 5a). Given that the observed westerly anomalies also had a secondary maximum in the troposphere in February 2021 (Fig. 5a), the control forecasts that missed the stratospheric westerly anomalies but hit the tropospheric westerly anomalies may imply that the summer westerly anomalies could be in part driven by tropospheric processes, possibly associated with La Niña (e.g., L'Heureux and Thompson 2006; Lim et al. 2016; Byrne et al. 2019). The good prediction of the westerly anomalies in DJF 2020-21 in the lower stratosphere and the troposphere then skilfully led to the prediction of a positive SAM in that summer at 3-month lead time despite the ozone forcing being climatological (Fig. 9d). The forecast also skilfully captured the higher-than-normal rainfall over the eastern part of south-eastern Australia at 3-month lead time (Fig. 9e), which is likely due to the model's ability to predict the positive SAM and associated circulations that bring rainfall to the region (Fig. S4). However, the positive rainfall was under-predicted. Also, the wet forecast was extended too far to the west of the south-eastern region compared to the observation, which seems partly due to the model bias in simulating the SAM and rainfall relationship in the western area (Fig. S4).

4.2 Experimental forecasts with the realistic ozone forcing of 2020-21

We presented in Figure 8 the lower-than-usual concentration of the Antarctic ozone observed in spring 2020 in the lower stratosphere and the resultant lower-than-usual ozone concentration near the Antarctic tropopause that persisted into the following autumn of 2021. When this low ozone was used to force the ACCESS-S2 system, the Antarctic lower stratosphere was forecast to be substantially colder during late spring and summer than that forced by the climatological ozone (Fig. 10 lower panels) by reducing the ultraviolet radiation absorption and associated short-wave heating (e.g.,

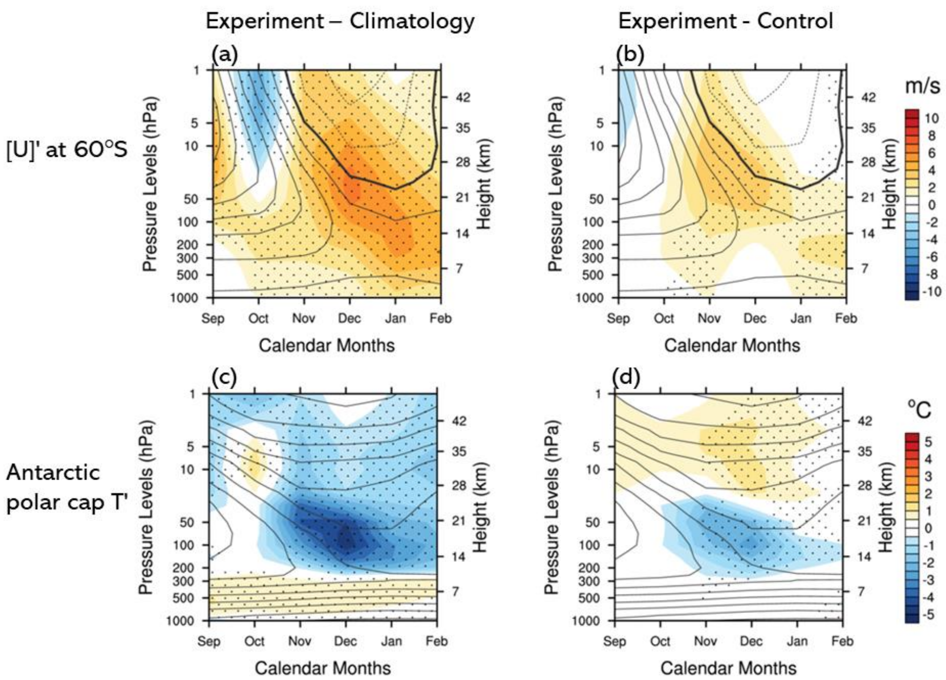

Figure 10. (Left panels) Experimental forecasts with the realistic ozone forcing of September 2020 – February 2021 for (a) [U]' at 60°S and (c) the Antarctic polar cap averaged T'. (Right panels) Differences made by the realistic ozone forcing compared to the climatological ozone forcing for (b) [U]' at 60°S and (d) the Antarctic polar cap averaged T'. In (a) and (c) the contours and stippling indicate the same as for Figure 9. In (b) and (d) the contours indicate the hindcast climatologies of [U] at 60°S and the Antarctic polar cap averaged T as for Figure 9, but the stippling denotes the statistically significant ensemble mean differences between the experimental and control forecasts with 33 samples in each set.

Keeble et al. 2014). Consistent with this temperature change, the experimental forecasts simulated a much stronger polar vortex during October to December 2020 in the stratosphere and stronger westerlies during the following January to February in the lower stratosphere and troposphere than the control forecasts (Fig. 10 upper panels), better matching the representation of the super vortex event in the reanalysis (Fig. 5a). In addition, the impact of the realistic ozone forcing appears to have reached the top of the stratosphere, making the forecast upper stratospheric zonal winds stronger in November at 40-80°S (Fig. 11b), thereby delaying the vortex breakdown, which is similar to what happened in 2020 (Fig. 5c).

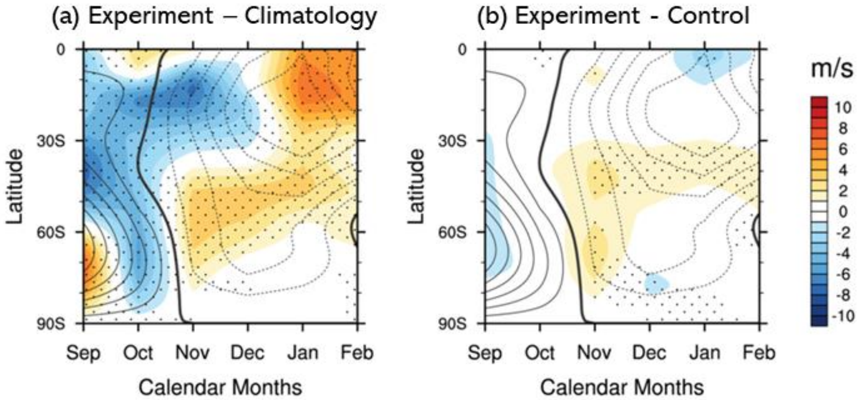

Figure 11. The same as Figure 10 except [U]' at 1 hPa.

Since the forecast spring polar vortex and its downward coupling strengthened with the realistic ozone forcing, a stronger positive SAM was predicted, especially with deeper low-pressure anomalies in the Antarctic region (Fig. 12). A clear improvement in predicting the dipole pressure anomalies is also seen in the southern Atlantic Ocean. Furthermore, the experimental forecasts with the 2020 ozone generated substantially higher rainfall over south-eastern Australia than the control forecasts with the climatological ozone, resulting in an improved forecast for the eastern part of south-eastern Australia but a false alarm for above-average rainfall for the western part (Fig. 13a). Statistically significant increases of rainfall generated by the realistic ozone forcing are found in the central part of south-eastern Australia (Fig. 13b), which is more or less consistent with where the observed SAM and rainfall relationship is prominent for 1981-2018 (Fig. 7b).

The improvements in predicting the polar stratospheric temperatures and vortex strength achieved by the realistic ozone forcing are statistically significant at the 90% confidence level, and the improvement in predicting the positive SAM in summer at the 3-month lead time is statistically significant at the 95% confidence level, as assessed by a two-tailed paired student t-test with 33 forecast members in each set. The improvement in the south-eastern Australian summer rainfall forecast at 3-month lead time is statistically significant at the 90% confidence level.

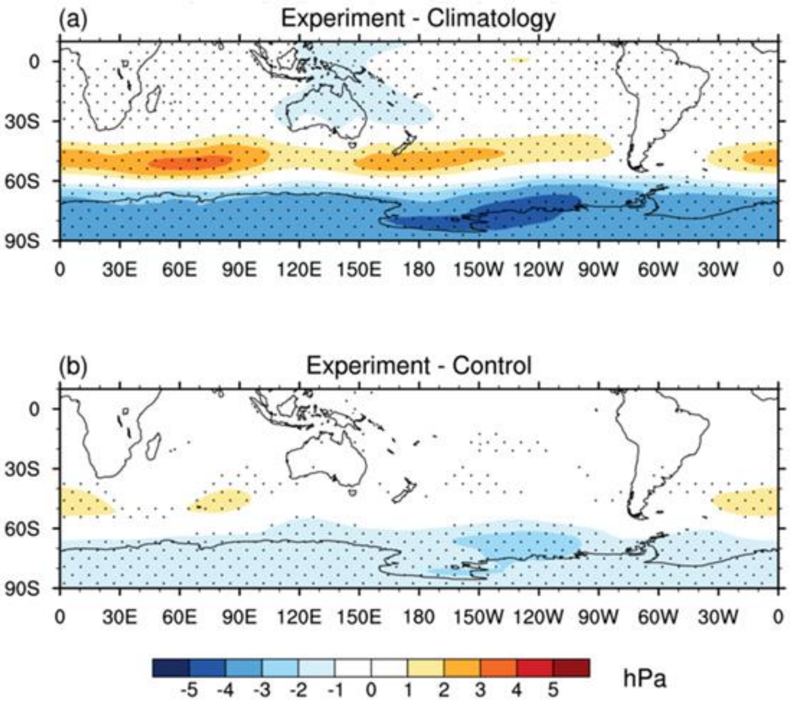

Figure 12. (a) Experimental forecasts with the realistic ozone forcing of 2020 for MSLP anomalies of DJF 2020-21 when the forecasts were initialised on 1 September 2020. (b) Differences made by the realistic ozone forcing compared to the climatological ozone forcing. The stippling indicates the statistical significance of the ensemble mean difference (a) between the experimental forecasts and the 1981-2018 hindcasts and (b) between the experimental forecasts and the control forecasts at the 90% confidence level, given 3x38 samples of the hindcasts and 33 samples of the control and experimental forecasts as described in Figures 9 and 10.

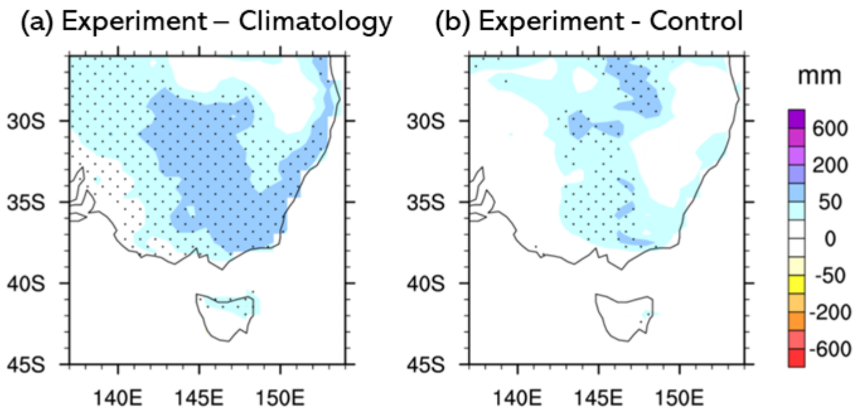

Figure 13. The same as Figure 12 except rainfall anomalies of DJF 2020-21 over south-eastern Australia.

5. Concluding Remarks

In the last four years, the Antarctic stratosphere experienced exceptionally large variability, with a near-record/record-breaking stratospheric polar vortex weakening and warming event in spring 2019, followed by three persistently strong and cold polar vortex events in the spring seasons of 2020, 2021, and 2022. Among these cold events, the 2020 polar vortex, measured at 60°S and 10 hPa in October-December, was the strongest and coldest on record in the mid- to lower stratosphere for the late spring season since the beginning of the satellite observation in 1979. However, this super vortex event was not skilfully predicted by the BoM's dynamical S2S forecast system until the wind and temperature anomalies of the vortex were already substantially large. Motivated by this forecast challenge, we have explored the characteristics of the 2020 super vortex event and associated surface climate conditions; and attempted to understand a possible reason for the lack of long-lead predictability of this vortex event and a potential role of realistic ozone forcing for the vortex strength and evolution and its downward coupling. We have tackled these research problems by conducting forecast sensitivity experiments to the climatological ozone *vs.* the realistic 2020 ozone forcing, having considered that realistic ozone forcing is missing in the BoM's dynamical S2S forecast systems, ACCESS-S1/S2.

Our results have shown that the 2020 super vortex event did not follow the usual linear dynamical processes, which involve wave-mean flow feedback and associated poleward transition of dipole anomalies of the winter stratospheric jet at the top of the stratosphere. In fact, the poleward shift of the jet and increased upward propagating wave activities in the SH extratropics in winter were suggestive of a polar vortex weakening and warming event in spring 2020. Although the occurrence of this strong vortex event was unexpected, its downward coupling was typical for such an event, resulting in a positive SAM at the surface in the following summer, which is likely to have promoted increased summer rainfall over the eastern part of south-eastern Australia.

The ACCESS-S2 33-member ensemble mean forecasts forced with the climatological ozone (control forecasts) fell short in predicting the stronger-than-normal October-December mean vortex measured at 60°S and 10 hPa at 1-month lead time. This was because the model simulated a poleward shift of the jet with the midlatitude easterly anomalies present at the beginning of September, which did not occur in reality. However, the control forecasts eventually simulated stronger-than-normal westerlies in the lower stratosphere to the troposphere in summer and a delayed vortex breakdown in the upper stratosphere, consistent with those represented in the reanalyses. Consequently, the positive SAM in the summer of 2020-21 was skilfully predicted even with the climatological ozone forcing. The experimental set of 33-member ensemble mean forecasts forced with the ERA-5 ozone of 2020 more skilfully simulated the unusually cold polar stratosphere and the unusually strong and persistent vortex in the spring and early summer of 2020, which led to better predictions of the positive SAM in the summer and associated wetter-than-normal conditions over the east of south-eastern Australia.

Overall, these findings on the role of ozone in the predictability of the tropospheric SAM and associated Australian rainfall are consistent with the results shown in previous studies (Thompson et al. 2005; Fogt et al. 2009; Kang et al. 2011; Son et al. 2013; Hendon et al. 2020; Oh et al. 2022). Our study reveals that ozone also plays an important role in shaping the temporal evolution of polar stratospheric temperature anomalies, and that the impact of using realistic ozone is not limited to the lower stratosphere where the ozone anomalies are concentrated but can reach into the upper stratosphere, therefore influencing the timing of the vortex breakdown. These novel results highlight the importance of ozone as a source of predictability yet to be exploited for S2S forecasts. Thus, we argue that future model development efforts should prioritise improving representations of ozone forcing for seasonal prediction systems through a novel parameterisation scheme or an affordable interactive chemistry scheme. On this note, it is worth mentioning a caveat that our forecast sensitivity experiments to prescribed climatological *vs*. observed ozone forcing demonstrate the predictability explained by the perfect knowledge of zonal-mean ozone; but if an interactive chemistry scheme is implemented in dynamical forecast systems, predictions of ozone would be linked to other forecast variables such as winds and temperatures and subsequent feedbacks. Therefore, in such a case, the maximum benefit of improving ozone forcing in dynamical forecasts will only be realised when forecast skill for the dynamics associated with the polar vortex and its downward coupling is reliably high.

Although we diagnosed the atypical evolution of the 2020 super vortex, which was not skilfully captured by the ACCESS-S2 system at 1-month lead time, a future study is needed to understand why the sudden development occurred; this will require in-depth investigation of the middle atmospheric dynamics in 2020. Another interesting subject to explore may be a possible contribution of La Niña to the different stages of the 2020 vortex life cycle and the surface SAM (Byrne et al. 2019), given the frequent concurrence of La Niña and unusually strong Antarctic stratospheric vortex events (e.g., in 1998-99, 2010-11 and 2020-2022) even though previous work did not show a significant linear relationship between canonical eastern Pacific-type El Niño and Antarctic stratospheric vortex variability (e.g., Hurwitz et al. 2011; Lim et al. 2018).

Acknowledgements

This study is part of the Victorian Water and Climate Initiative (VicWaCI), funded by the Department of the Energy, Environment, and Climate Action; the National Environmental Science Program (NESP), funded by the Department of Climate Change, Energy, the Environment and Water; and the Australian Research Council Special Research Initiative for Securing Antarctica's Environmental Future (SAEF) Program (SR200100005). S. A. acknowledges the Australian Research Council's Discovery Project (DP220101468). J. M. A. was partially supported by the Regional and Global Model Analysis component of the Earth and Environmental System Modeling Program of the U.S. Department of Energy's Office of Biological and Environmental Research via National Science Foundation IA 1947282. S.-W. S. was supported by the Korea Environment Industry &Technology Institute (KEITI) through "Climate Change R&D Project for New Climate Regime.", funded by the Korea Ministry of Environment (MOE) (2022003560004). G. L. Manney was supported by the Jet Propulsion Laboratory (JPL) Microwave Limb Sounder team under JPL subcontract #1521127 to NWRA, and by NSF Climate and Large-scale Dynamics Grant #2015906. This research was undertaken on the NCI National Facility in Canberra, Australia, which is supported by the Australian Commonwealth Government. The authors thank Ms Jo Croucher and Drs Yiling Liu and Heather Leasor at the NCI for their great efforts to make the BoM forecast data publicly available on the NCI data server. The NCAR Command Language (NCL; http://www.ncl.ucar.edu) version and Python version 2.7.16 were used for data analysis and visualization of the results. We acknowledge the Japanese Meteorological Agency, NCAR/UCAR, ECMWF, and BoM for producing/archiving the JRA-55 reanalysis, the ERA5 reanalysis, and the Australian gridded climate data, respectively. We also acknowledge the NOAA CPC, the British Antarctic Survey, and the NASA for the availability of the Antarctic Oscillation index, an observation-based SAM index, and the Antarctic total column ozone data, respectively. The authors want to thank Drs. Debra Hudson and Ghyslaine Boschat at the BoM for their valuable and constructive feedback on the manuscript.

Open Research

Data Availability Statement

The JRA-55 monthly mean reanalysis set is available at NCAR Research Data Archive (ucar.edu). The ERA5 monthly ozone reanalysis data are available at https://cds.climate.copernicus.eu/cdsapp#!/dataset/reanalysis-era5-single-levels-monthly-means?tab=overview. The Antarctic Oscillation Index is available at https://www.cpc.ncep.noaa.gov/products/precip/CWlink/daily_ao_index/aao/aao.shtml. Marshall (2003)'s observation-based SAM index is available at http://www.nerc-bas.ac.uk/icd/gjma/sam.html. The Antarctic total column ozone data are from the NASA Ozone Watch (https://ozonewatch.gsfc.nasa.gov/SH.html). The Australian gridded climate data are available at http://www.bom.gov.au/climate/data/. The BoM hindcast and control and experimental forecast data are available at https://doi.org/10.25914/8fdt-6v74. The NCL software resources are available at https://www.ncl.ucar.edu/.

References

Andrews, D. G., Holton, J. R., & Leovy, C. B. (1987). *Middle Atmosphere Dynamics*. Academic Press, Inc.

Baldwin, M. P., Ayarzagüena, B., Birner, T., Butchart, N., Butler, A. H., Charlton-Perez, A. J., Domeisen, D. I. V., Garfinkel, C. I., Garny, H., Gerber, E. P., Hegglin, M. I., Langematz, U., & Pedatella, N. M. (2021). Sudden Stratospheric Warmings. *Reviews of Geophysics*, *59*(1). https://doi.org/10.1029/2020RG000708

Black, R. X., & McDaniel, B. A. (2007). Interannual Variability in the Southern Hemisphere Circulation Organized by Stratospheric Final Warming Events. *Journal of the Atmospheric Sciences*, *64*(8), 2968–2974. https://doi.org/10.1175/JAS3979.1

Bureau of Meteorology. (2019). APS3 upgrade of the ACCESS-G/GE Numerical Weather Prediction System. *National Operational Centre Operations Bulletin Number 125*.

Byrne, N. J., & Shepherd, T. G. (2018). Seasonal Persistence of Circulation Anomalies in the Southern Hemisphere Stratosphere and Its Implications for the Troposphere. *Journal of Climate*, *31*(9), 3467–3483. https://doi.org/10.1175/JCLI-D-17-0557.1

Byrne, N. J., Shepherd, T. G., & Polichtchouk, I. (2019). Subseasonal-to-Seasonal Predictability of the Southern Hemisphere Eddy-Driven Jet During Austral Spring and Early Summer. *Journal of Geophysical Research: Atmospheres*, *124*(13), 2018JD030173. https://doi.org/10.1029/2018JD030173

Cionni, I., Eyring, V., Lamarque, J. F., Randel, W. J., Stevenson, D. S., Wu, F., Bodeker, G. E., Shepherd, T. G., Shindell, D. T., & Waugh, D. W. (2011). Ozone database in support of CMIP5 simulations: results and corresponding radiative forcing. *Atmospheric Chemistry and Physics*, *11*(21), 11267–11292. https://doi.org/10.5194/acp-11-11267-2011

Dee, D. P., Uppala, S. M., Simmons, A. J., Berrisford, P., Poli, P., Kobayashi, S., Andrae, U., Balmaseda, M. A., Balsamo, G., Bauer, P., Bechtold, P., Beljaars, A. C. M., van de Berg, L., Bidlot, J., Bormann, N., Delsol, C., Dragani, R., Fuentes, M., Geer, A. J., … Vitart, F. (2011). The ERA-Interim reanalysis: configuration and performance of the data assimilation system. *Quarterly Journal of the Royal Meteorological Society*, *137*(656), 553–597. https://doi.org/10.1002/qj.828

Evans, A., Jones, D., Smalley, R., & Lellyett, S. (2020). An enhanced gridded rainfall dataset scheme for Australia. In *Bureau Research Report No. 41* (Issue June). https://www.google.com.au/search?q=An+enhanced+gridded+rainfall+analysis+scheme+for+Australia&rls=com.microsoft%3Aen-GB%3A%7Breferrer%3Asource%7D&sxsrf=ALiCzsbui9q6NgSQW0jYNPHo_q7dSMvDnQ%3A1662425730786&ei=gpoWY9PVL4SdseMPjuym4A0&ved=0ahUKEwjTnpi5-v75AhWE

Fogt, R. L., & Marshall, G. J. (2020). The Southern Annular Mode: Variability, trends, and climate impacts across the Southern Hemisphere. *Wiley Interdisciplinary Reviews: Climate Change*, *11*(4), 1–24. https://doi.org/10.1002/wcc.652

Fogt, R. L., Perlwitz, J., Pawson, S., & Olsen, M. A. (2009). Intra-annual relationships between polar ozone and the SAM. *Geophysical Research Letters*, *36*(4), 1–6. https://doi.org/10.1029/2008GL036627

Friedel, M., Chiodo, G., Stenke, A., Domeisen, D. I. V., Fueglistaler, S., Anet, J. G., & Peter, T. (2022). Springtime arctic ozone depletion forces northern hemisphere climate anomalies. *Nature Geoscience*, *15*(7), 541–547. https://doi.org/10.1038/s41561-022-00974-7

Gillett, N. P., Kell, T. D., & Jones, P. D. (2006). Regional climate impacts of the Southern Annular Mode. *Geophysical Research Letters*, *33*(23), L23704. https://doi.org/10.1029/2006GL027721

Gong, D., & Wang, S. (1999). Definition of Antarctic Oscillation index. *Geophysical Research Letters*, *26*(4), 459–462. https://doi.org/10.1029/1999GL900003

Hartmann, D. L. (2022). The Antarctic ozone hole and the pattern effect on climate sensitivity. *Proceedings of the National Academy of Sciences of the United States of America*, *119*(35), 1–5. https://doi.org/10.1073/pnas.2207889119

Hartmann, D. L., Mechoso, C. R., & Yamazaki, K. (1984). Observations of Wave-Mean Flow Interaction in the Southern Hemisphere. In *Journal of Atmospheric Sciences* (Vol. 41, Issue 3, pp. 351–362). https://doi.org/10.1175/1520-0469(1984)041<0351:OOWMFI>2.0.CO;2

Heidemann, H., Cowan, T., Henley, B. J., Ribbe, J., Freund, M., & Power, S. (2023). Variability and long-term change in Australian monsoon rainfall: A review. *Wiley Interdisciplinary Reviews: Climate Change*, *January 2022*, 1–28. https://doi.org/10.1002/wcc.823

Hendon, H. H., Lim, E.-P., Arblaster, J. M., & Anderson, D. L. T. (2014). Causes and predictability of the record wet east Australian spring 2010. *Climate Dynamics*, *42*(5–6), 1155–1174. https://doi.org/10.1007/s00382-013-1700-5

Hendon, H. H., Lim, E. -P., & Abhik, S. (2020). Impact of Interannual Ozone Variations on the

Downward Coupling of the 2002 Southern Hemisphere Stratospheric Warming. *Journal of Geophysical Research: Atmospheres*, *October 2002*, 1–16. https://doi.org/10.1029/2020JD032952

Hendon, H. H., Thompson, D. W. J., & Wheeler, M. C. (2007). Australian rainfall and surface temperature variations associated with the Southern Hemisphere annular mode. *Journal of Climate*, *20*(11), 2452–2467. https://doi.org/10.1175/JCLI4134.1

Henley, B. J., Gergis, J., Karoly, D. J., Power, S., Kennedy, J., & Folland, C. K. (2015). A Tripole Index for the Interdecadal Pacific Oscillation. *Climate Dynamics*, *45*(11–12), 3077–3090. https://doi.org/10.1007/s00382-015-2525-1

Hersbach, H., Bell, B., Berrisford, P., Hirahara, S., Horányi, A., Muñoz-Sabater, J., Nicolas, J., Peubey, C., Radu, R., Schepers, D., Simmons, A., Soci, C., Abdalla, S., Abellan, X., Balsamo, G., Bechtold, P., Biavati, G., Bidlot, J., Bonavita, M., … Thépaut, J. N. (2020). The ERA5 global reanalysis. *Quarterly Journal of the Royal Meteorological Society*, *146*(730), 1999–2049. https://doi.org/10.1002/qj.3803

Hio, Y., & Yoden, S. (2004). Quasi-Periodic Variations of the Polar Vortex in the Southern Hemisphere Stratosphere Due to Wave–Wave Interaction. *Journal of the Atmospheric Sciences*, *61*(21), 2510–2527. https://doi.org/10.1175/JAS3257.1

Hio, Y., & Yoden, S. (2005). Interannual Variations of the Seasonal March in the Southern Hemisphere Stratosphere for 1979–2002 and Characterization of the Unprecedented Year 2002. *Journal of the Atmospheric Sciences*, *62*(3), 567–580. https://doi.org/10.1175/JAS-3333.1

Hudson et. al., D. (2017). ACCESS-S1 The new Bureau of Meteorology multi-week to seasonal prediction system. *Journal of Southern Hemisphere Earth System Science*, *67*(3), 132–159. https://doi.org/10.22499/3.6703.001

Hurwitz, M. M., Newman, P. A., Oman, L. D., & Molod, A. M. (2011). Response of the Antarctic Stratosphere to Two Types of El Niño Events. *Journal of the Atmospheric Sciences*, *68*(4), 812–822. https://doi.org/10.1175/2011JAS3606.1

Jones, D. A., Wang, W., & Fawcett, R. (2009). High-quality spatial climate data-sets for Australia. *Australian Meteorological and Oceanographic Journal*, *58*, 233–248.

Kang, S. M., Polvani, L. M., Fyfe, J. C., & Sigmond, M. (2011). Impact of polar ozone depletion on subtropical precipitation. *Science*, *332*(2011), 951–954. https://doi.org/10.1126/science.1202131

Keeble, J., Braesicke, P., Abraham, N. L., Roscoe, H. K., & Pyle, J. A. (2014). The impact of polar stratospheric ozone loss on southern Hemisphere stratospheric circulation and climate.

Atmospheric Chemistry and Physics, *14*(24), 13705–13717. https://doi.org/10.5194/acp-14-13705-2014

Kidson, J. W. (1988). Indices of the Southern Hemisphere Zonal Wind. In *Journal of Climate* (Vol. 1, Issue 2, pp. 183–194). https://doi.org/10.1175/1520-0442(1988)001<0183:IOTSHZ>2.0.CO;2

Kobayashi, S., Ota, Y., Harada, Y., Ebita, A., Moriya, M., Onoda, H., Onogi, K., Kamahori, H., Kobayashi, C., Endo, H., Miyaoka, K., & Takahashi, K. (2015). The JRA-55 Reanalysis: General Specifications and Basic Characteristics. *Journal of the Meteorological Society of Japan. Ser. II*, *93*(1), 5–48. https://doi.org/10.2151/jmsj.2015-001

Kosaka, Y., & Xie, S.-P. (2013). Recent global-warming hiatus tied to equatorial Pacific surface cooling. *Nature*, *501*(7467), 403–407. https://doi.org/10.1038/nature12534

Kuroda, Y., & Kodera, K. (1998). Interannual variability in the troposphere and stratosphere of the Southern Hemisphere winter. *Journal of Geophysical Research: Atmospheres*, *103*(D12), 13787–13799. https://doi.org/10.1029/98JD01042

L'Heureux, M. L., & Thompson, D. W. J. (2006). Observed relationships between the El Niño–Southern Oscillation and the extratropical zonal-mean circulation. *Journal of Climate*, *19*(2), 276–287. https://doi.org/10.1175/JCLI3617.1

Levelt, P. F., van den Oord, G. H. J., Dobber, M. R., Malkki, A., Huib Visser, Johan de Vries, Stammes, P., Lundell, J. O. V., & Saari, H. (2006). The ozone monitoring instrument. *IEEE Transactions on Geoscience and Remote Sensing*, *44*(5), 1093–1101. https://doi.org/10.1109/TGRS.2006.872333

Lim, E.-P., & Hendon, H. H. (2015). Understanding and predicting the strong Southern Annular Mode and its impact on the record wet east Australian spring 2010. *Climate Dynamics*, *44*(9–10), 2807–2824. https://doi.org/10.1007/s00382-014-2400-5

Lim, E.-P., Hendon, H. H., Arblaster, J. M., Chung, C., Moise, A. F., Hope, P., Young, G., & Zhao, M. (2016). Interaction of the recent 50 year SST trend and La Niña 2010: amplification of the Southern Annular Mode and Australian springtime rainfall. *Climate Dynamics*, *47*(7–8), 2273–2291. https://doi.org/10.1007/s00382-015-2963-9

Lim, E.-P., Hendon, H. H., Boschat, G., Hudson, D., Thompson, D. W. J., Dowdy, A. J., & Arblaster, J. M. (2019). Australian hot and dry extremes induced by weakenings of the stratospheric polar vortex. *Nature Geoscience*, *12*(11), 896–901. https://doi.org/10.1038/s41561-019-0456-x

Lim, E.-P., Hendon, H. H., & Thompson, D. W. J. (2018). Seasonal evolution of stratosphere-troposphere coupling in the Southern Hemisphere and implications for the predictability of surface climate. *Journal of Geophysical Research: Atmospheres*, *123*, 12,002–12,016. https://doi.org/10.1029/2018JD029321

Lim, E. P., Hendon, H. H., Butler, A. H., Thompson, D. W. J., Lawrence, Z. D., Scaife, A. A., Shepherd, T. G., Polichtchouk, I., Nakamura, H., Kobayashi, C., Comer, R., Coy, L., Dowdy, A., Garreaud, R. D., Newman, P. A., & Wang, G. (2021). Supplementary Material - The 2019 southern hemisphere stratospheric polar vortex weakening and its impacts. *Bulletin of the American Meteorological Society*, *102*(6), E1150–E1171. https://doi.org/10.1175/BAMS-D-20-0112.1

Limpasuvan, V., Hartmann, D. L., Thompson, D. W. J., Jeev, K., & Yung, Y. L. (2005). Stratosphere-troposphere evolution during polar vortex intensification. *Journal of Geophysical Research*, *110*(D24), D24101. https://doi.org/10.1029/2005JD006302

MacLachlan, C., Arribas, A., Peterson, K. A., Maidens, A., Fereday, D., Scaife, A. A., Gordon, M., Vellinga, M., Williams, A., Comer, R. E., Camp, J., Xavier, P., & Madec, G. (2015). Global Seasonal forecast system version 5 (GloSea5): a high-resolution seasonal forecast system. *Quarterly Journal of the Royal Meteorological Society*, *141*(689), 1072–1084. https://doi.org/10.1002/qj.2396

Marshall, G. J. (2003). Trends in the Southern Annular Mode from observations and reanalyses. *Journal of Climate*, *16*(24), 4134–4143. https://doi.org/10.1175/1520-0442(2003)016<4134:TITSAM>2.0.CO;2

Matsuno, T. (1970). Vertical Propagation of Stationary Planetary Waves in the Winter Northern Hemisphere. *Journal of the Atmospheric Sciences*, *27*(6), 871–883. https://doi.org/10.1175/1520-0469(1970)027<0871:VPOSPW>2.0.CO;2

McBride, J. L., & Nicholls, N. (1983). Seasonal Relationships between Australian Rainfall and the Southern Oscillation. *Monthly Weather Review*, *111*(10), 1998–2004. https://doi.org/10.1175/1520-0493(1983)111<1998:SRBARA>2.0.CO;2

Noguchi, S., Kuroda, Y., Kodera, K., & Watanabe, S. (2020). Robust Enhancement of Tropical Convective Activity by the 2019 Antarctic Sudden Stratospheric Warming. *Geophysical Research Letters*, *47*(15). https://doi.org/10.1029/2020GL088743

North, G. R., Bell, T. L., Cahalan, R. F., & Moeng, F. J. (1982). Sampling Errors in the Estimation of Empirical Orthogonal Functions. *Monthly Weather Review*, *110*(7), 699–706. https://doi.org/10.1175/1520-0493(1982)110<0699:seiteo>2.0.co;2

Oh, J., Son, S. W., Choi, J., Lim, E. P., Garfinkel, C., Hendon, H., & Kim, Y. (2022). Impact of stratospheric ozone on the subseasonal prediction in the southern hemisphere spring. *Progress in*

Earth and Planetary Science. https://doi.org/10.1186/s40645-022-00485-4

Polvani, L. M., & Waugh, D. W. (2004). Upward wave activity flux as a precursor to extreme stratospheric events and subsequent anomalous surface weather regimes. *Journal of Climate*, *17*(18), 3548–3554. https://doi.org/10.1175/1520-0442(2004)017<3548:UWAFAA>2.0.CO;2

Randel, W. J., & Newman, P. A. (1998). The Stratosphere in the Southern Hemisphere. In *Meteorology of the Southern Hemisphere* (pp. 243–282). American Meteorological Society. https://doi.org/10.1007/978-1-935704-10-2_9

Rao, J., Garfinkel, C. I., White, I. P., & Schwartz, C. (2020). The Southern Hemisphere Minor Sudden Stratospheric Warming in September 2019 and its Predictions in S2S Models. *Journal of Geophysical Research: Atmospheres*, *125*(14), 1–19. https://doi.org/10.1029/2020JD032723

Reason, C. J. C., & Rouault, M. (2005). Links between the Antarctic Oscillation and winter rainfall over western South Africa. *Geophysical Research Letters*, *32*(7), 1–4. https://doi.org/10.1029/2005GL022419

Rieger, L. A., Randel, W. J., Bourassa, A. E., & Solomon, S. (2021). Stratospheric Temperature and Ozone Anomalies Associated With the 2020 Australian New Year Fires. *Geophysical Research Letters*, *48*(24), 1–8. https://doi.org/10.1029/2021GL095898

Risbey, J. S., Pook, M. J., McIntosh, P. C., Wheeler, M. C., & Hendon, H. H. (2009). On the remote drivers of rainfall variability in Australia. *Monthly Weather Review*, *137*(10), 3233–3253. https://doi.org/10.1175/2009MWR2861.1

Salby, M., Titova, E., & Deschamps, L. (2011). Rebound of antarctic ozone. *Geophysical Research Letters*, *38*(9), 2–5. https://doi.org/10.1029/2011GL047266

Santee, M. L., Lambert, A., Manney, G. L., Livesey, N. J., Froidevaux, L., Neu, J. L., Schwartz, M. J., Millán, L. F., Werner, F., Read, W. G., Park, M., Fuller, R. A., & Ward, B. M. (2022). Prolonged and Pervasive Perturbations in the Composition of the Southern Hemisphere Midlatitude Lower Stratosphere From the Australian New Year's Fires. *Geophysical Research Letters*, *49*(4), 1–11. https://doi.org/10.1029/2021GL096270

Sen Gupta, A., & England, M. H. (2006). Coupled ocean-atmosphere-ice response to variations in the southern annular mode. *Journal of Climate*, *19*(18), 4457–4486. https://doi.org/10.1175/JCLI3843.1

Seviour, W. J. M., Hardiman, S. C., Gray, L. J., Butchart, N., MacLachlan, C., & Scaife, A. A. (2014). Skillful seasonal prediction of the Southern Annular Mode and Antarctic ozone. *Journal of Climate*, *27*(19), 7462–7474. https://doi.org/10.1175/JCLI-D-14-00264.1

Sharmila, S., & Hendon, H. H. (2020). Mechanisms of multiyear variations of Northern Australia wet-season rainfall. *Scientific Reports*, *10*(1), 1–11. https://doi.org/10.1038/s41598-020-61482-5

Shaw, T. A., Perlwitz, J., & Harnik, N. (2010). Downward wave coupling between the stratosphere and troposphere: The importance of meridional wave guiding and comparison with zonal-mean coupling. *Journal of Climate*, *23*(23), 6365–6381. https://doi.org/10.1175/2010JCLI3804.1

Shen, X., Wang, L., & Osprey, S. (2020). Tropospheric Forcing of the 2019 Antarctic Sudden Stratospheric Warming. *Geophysical Research Letters*, *47*(20), 1–8. https://doi.org/10.1029/2020GL089343

Shen, X., Wang, L., Osprey, S., Hardiman, S. C., Scaife, A. A., & Ma, A. J. I. (2022). The Life Cycle and Variability of Antarctic Weak Polar Vortex Events. *Journal of Climate*, *35*(6), 2075–2092. https://doi.org/10.1175/JCLI-D-21-0500.1

Shiotani, M., Shimoda, N., & Hirota, I. (1993). Interannual variability of the stratospheric circulation in the Southern Hemisphere. *Quarterly Journal of the Royal Meteorological Society*, *119*(511), 531–546.

Silvestri, G. E., & Vera, C. S. (2003). Antarctic Oscillation signal on precipitation anomalies over southeastern South America. *Geophysical Research Letters*, *30*(21), 2115. https://doi.org/10.1029/2003GL018277

Simmons, A., Soci, C., Nicolas, J., Bell, B., Berrisford, P., Dragani, R., Flemming, J., Haimberger, L., Healy, S., & Hersbach, H. (2020). *Technical Memo ECMWF*. *January*.

Solomon, S., Ivy, D. J., Kinnison, D., Mills, M. J., Iii, R. R. N., & Schmidt, A. (2016). *Emergence of healing in the Antarctic ozone layer*. *0061*.

Solomon, S., Stone, K., Yu, P., Murphy, D. M., Kinnison, D., Ravishankara, A. R., & Wang, P. (2023). Chlorine activation and enhanced ozone depletion induced by wildfire aerosol. *Nature*, *615*(7951), 259–264. https://doi.org/10.1038/s41586-022-05683-0

Son, S. W., Purich, A., Hendon, H. H., Kim, B. M., & Polvani, L. M. (2013). Improved seasonal forecast using ozone hole variability? Supplementary Info. *Geophysical Research Letters*, *40*(23), 6231–6235. https://doi.org/10.1002/2013GL057731

SPARC. (2022). SPARC Reanalysis Intercomparison Project (S-RIP) Final Report. In M. Fujiwara, G. L. Manney, L. J. Gray, & J. S. Wright (Eds.), *SPARC Report No. 10/WCRP Report 6/2021*. https://doi.org/10.17874/800dee57d13

Stammerjohn, S. E., Martinson, D. G., Smith, R. C., Yuan, X., & Rind, D. (2008). Trends in Antarctic annual sea ice retreat and advance and their relation to El Niño-Southern Oscillation and

Southern Annular Mode variability. *Journal of Geophysical Research: Oceans*, *113*(3), 1–20. https://doi.org/10.1029/2007jc004269

Stolarski, R. S., McPeters, R. D., & Newman, P. a. (2005). The Ozone Hole of 2002 as Measured by TOMS. *Journal of the Atmospheric Sciences*, *62*(3), 716–720. https://doi.org/10.1175/JAS-3338.1

Stone, K. A., Solomon, S., Kinnison, D. E., & Mills, M. J. (2021). On Recent Large Antarctic Ozone Holes and Ozone Recovery Metrics. *Geophysical Research Letters*, *48*(22). https://doi.org/10.1029/2021GL095232

Thompson, D. W. J., Baldwin, M. P., & Solomon, S. (2005). Stratosphere–troposphere coupling in the Southern Hemisphere. *Journal of the Atmospheric Sciences*, *62*(3), 708–715. https://doi.org/10.1175/JAS-3321.1

Thompson, D. W. J., & Wallace, J. M. (2000). Annular modes in the extratropical circulation. Part I: Month-to-month variability. *Journal of Climate*, *13*(5), 1000–1016. https://doi.org/10.1175/1520-0442(2000)013<1000:AMITEC>2.0.CO;2

Walters, D., Boutle, I., Brooks, M., Melvin, T., Stratton, R., Vosper, S., Wells, H., Williams, K., Wood, N., Allen, T., Bushell, A., Copsey, D., Earnshaw, P., Edwards, J., Gross, M., Hardiman, S., Harris, C., Heming, J., Klingaman, N., … Xavier, P. (2017). The Met Office Unified Model Global Atmosphere 6.0/6.1 and JULES Global Land 6.0/6.1 configurations. *Geoscientific Model Development*, *10*(4), 1487–1520. https://doi.org/10.5194/gmd-10-1487-2017

Wang, G., Hendon, H. H., Arblaster, J. M., Lim, E. P., Abhik, S., & van Rensch, P. (2019). Compounding tropical and stratospheric forcing of the record low Antarctic sea-ice in 2016. *Nature Communications*, *10*(1), 13. https://doi.org/10.1038/s41467-018-07689-7

Wargan, K., Weir, B., Manney, G. L., Cohn, S. E., & Livesey, N. J. (2020). The Anomalous 2019 Antarctic Ozone Hole in the GEOS Constituent Data Assimilation System With MLS Observations. *Journal of Geophysical Research: Atmospheres*, *125*(18), 1–28. https://doi.org/10.1029/2020JD033335

Waters, J., Lea, D. J., Martin, M. J., Mirouze, I., Weaver, A., & While, J. (2015). Implementing a variational data assimilation system in an operational 1/4 degree global ocean model. *Quarterly Journal of the Royal Meteorological Society*, *141*(687), 333–349. https://doi.org/10.1002/qj.2388

Waters, J. W., Froidevaux, L., Harwood, R. S., Jarnot, R. F., Pickett, H. M., Read, W. G., Siegel, P. H., Cofield, R. E., Filipiak, M. J., Flower, D. A., Holden, J. R., Lau, G. K., Livesey, N. J., Manney, G. L., Pumphrey, H. C., Santee, M. L., Wu, D. L., Cuddy, D. T., Lay, R. R., … Walch,

M. J. (2006). The Earth observing system microwave limb sounder (EOS MLS) on the aura Satellite. *IEEE Transactions on Geoscience and Remote Sensing*, *44*(5), 1075–1092. https://doi.org/10.1109/TGRS.2006.873771

Wedd, R., Alves, O., de Burgh-Day, C., Down, C., Griffiths, M., Hendon, H. H., Hudson, D., Li, S., Lim, E.-P., Marshall, A. G., Shi, L., Smith, P., Smith, G., Spillman, C. M., Wang, G., Wheeler, M. C., Yan, H., Yin, Y., Young, G., … Zhou, X. (2022). ACCESS-S2: the upgraded Bureau of Meteorology multi-week to seasonal prediction system. *Journal of Southern Hemisphere Earth Systems Science*, *72*(3), 218–242. https://doi.org/10.1071/ES22026

Yook, S., Thompson, D. W. J., & Solomon, S. (2022). Climate Impacts and Potential Drivers of the Unprecedented Antarctic Ozone Holes of 2020 and 2021. *Geophysical Research Letters*, *49*(10). https://doi.org/10.1029/2022gl098064

Yu, P., Davis, S. M., Toon, O. B., Portmann, R. W., Bardeen, C. G., Barnes, J. E., Telg, H., Maloney, C., & Rosenlof, K. H. (2021). Persistent Stratospheric Warming Due to 2019–2020 Australian Wildfire Smoke - Supplementary Information. *Geophysical Research Letters*, *48*(7). https://doi.org/10.1029/2021GL092609

Yuan Zhang, Wallace, J. M., & Battisti, D. S. (1997). ENSO-like interdecadal variability: 1900-93. *Journal of Climate*, *10*(5), 1004–1020. https://doi.org/10.1175/1520-0442(1997)010<1004:eliv>2.0.co;2